PHYSICAL REVIEW E **73**, 020401(R) (2006)

Solvation forces between colloidal nanoparticles: Directed alignment

Yong Qin and Kristen A. Fichthorn*
Department of Chemical Engineering, The Pennsylvania State University, University Park, Pennsylvania 16802, USA
(Received 22 July 2005; revised manuscript received 2 December 2005; published 13 February 2006)

We study the solvation forces between colloidal nanoparticles in Lennard-Jones liquids using molecular-dynamics simulations. We find that due to the interplay between solvent ordering and surface structure, the solvation forces between two nanoparticles can vary between attraction and repulsion as the particles are rotated relative to one another at a fixed separation. These solvent-mediated forces tend to align the nanoparticles so that they rotate to approach one another in a solution via preferred pathways. This directed alignment could play a role in the assembly of macromolecules and nanoparticles in solution.

DOI: 10.1103/PhysRevE.73.020401 PACS number(s): 82.70.Dd, 81.07.−b, 81.16.Dn, 82.70.Uv

When two colloidal particles come within nanometer distances in a liquid solvent, the solvent can mediate a force between them. This solvation force (or hydration force, if the solvent is water) is due to differences between the solvent ordering and/or density in the gap between the particles and in the bulk liquid region around them [1]. Solvation forces have been quantified experimentally with the surface forces apparatus (SFA) and atomic force microscopy (AFM) [2–10], as well as with computer simulations [11–17]. These studies have shown that solvation forces could be more significant than van der Waals forces and, thus these forces could play a role in colloidal assembly and stability. Indeed, solvent-mediated hydrophobic forces have long been believed to play a major role in protein assembly and folding [18–23]. However, these forces and their origins have been notoriously difficult to quantify experimentally [8–10,22]. Simulation studies are hindered by the wide range of length and time scales involved [23], and, thus, the exact role of solvation forces remains elusive.

In this Rapid Communication, we present evidence that solvation forces can play an important and underappreciated role in colloidal systems, that of aligning colloidal objects in solution. We utilized classical molecular dynamics (MD) simulations to study the solvation forces between model colloidal nanoparticles in a Lennard-Jones (LJ) solvent. These model nanoparticles, just as actual colloidal particles, differ from the experimental scenarios probed in the SFA and AFM in two important ways. First, the particles are free to change their orientation relative to one another in solution, while the surfaces in experiments are fixed. Second, because of their finite size, even perfect crystalline particles possess distinct structural features (i.e., faces, edges, and vertices) that can be regarded as a form of surface roughness. Experimental studies of mesoscopic surfaces indicate that solvation forces are weaker for rough surfaces than smooth ones [4,8,9] and theoretical and computer-simulation studies indicate that these experimental results are due to a reduction in solvent ordering between rough surfaces [14–17]. Our simulations of colloidal nanoparticles [24], as well as theoretical and computer simulation studies of proteins [25], water near curved surfaces [26], and polymers [27] address smaller length scales than the experiments. These studies indicate that solvent ordering and solvation forces are not necessarily weaker for nanotextured surfaces, but they do show a sensitivity to local structural features of the surface. Here we show that nanoparticle reorientation due to local solvation forces induced by surface structure is significant and that it could play an important role in the stability and assembly of colloidal nanoparticles, polymers, and proteins.

Our model systems consist of two solid nanoparticles immersed in liquid solvent in the *NVT* ensemble. To acquire a general understanding, the solvent is simulated as a LJ liquid with the interaction truncated at a distance of 2.5σ. The reduced number density ρ^* and temperature T^* of the solvent are 0.7 and 1.0, respectively. Computer simulations of the SFA reveal that LJ liquids reproduce general trends seen in experiment [11]. Indeed, theories of hydrophobic hydration can explain experimental trends without including hydrogen bonding and its associated networking of water molecules [19–21]. The solid nanoparticles are modeled as rigid, atomic clusters. Two types of nanoparticles are considered: a 55-atom icosahedral crystal [28] and a 64-atom rough, amorphous sphere formed by simulated condensation of a LJ liquid. These are solvent-loving ("solvophilic") nanoparticles, in which the LJ solid-liquid interaction (ϵ_{sl}) is taken to be five times stronger than the LJ liquid-liquid interaction (ϵ_{ll}). Our results were mostly obtained using 3000 solvent atoms. The system size dependence of our results has been tested in simulations using 10 000–100 000 atoms and no significant differences were found.

We performed two types of MD simulations. In the first set of simulations, we maintained the nanoparticles at a fixed orientation relative to one another. In these simulations, the nanoparticle atoms are held as fixed interaction centers and we only simulate the motion of the solvent. We considered eight different nanoparticle orientations for the crystals and six for the rough spheres. In the second set of simulations, we relaxed each of the nanoparticle pair configurations from the first set by allowing the nanoparticles to rotate about their centers of mass under the impact of solvation forces. Thus, in the second set of simulations, we consider both solvent mo-

*Also at Department of Physics, The Pennsylvania State University, University Park, PA 16802. Electronic address: fichthorn@psu.edu

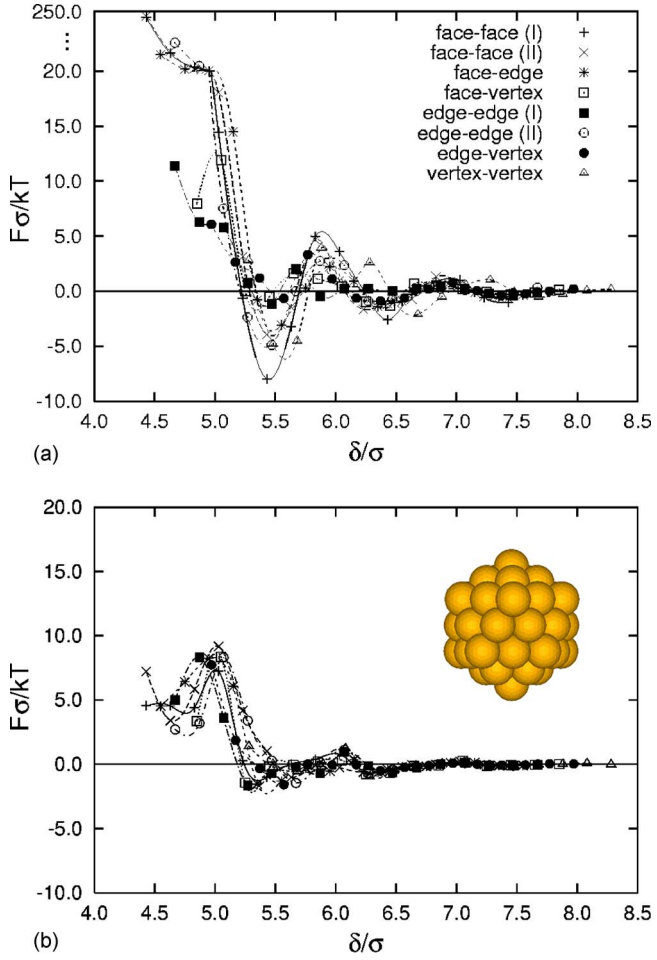

FIG. 1. (Color online) Solvation-force profiles for the crystalline nanoparticles [see inset of (b)] fixed at their initial configurations (a) and freely rotating about their centers of mass (b) under the impact of solvation forces and beginning with their initial configuration in (a). Variations between the forces at a fixed separation in (b) indicate the uncertainty.

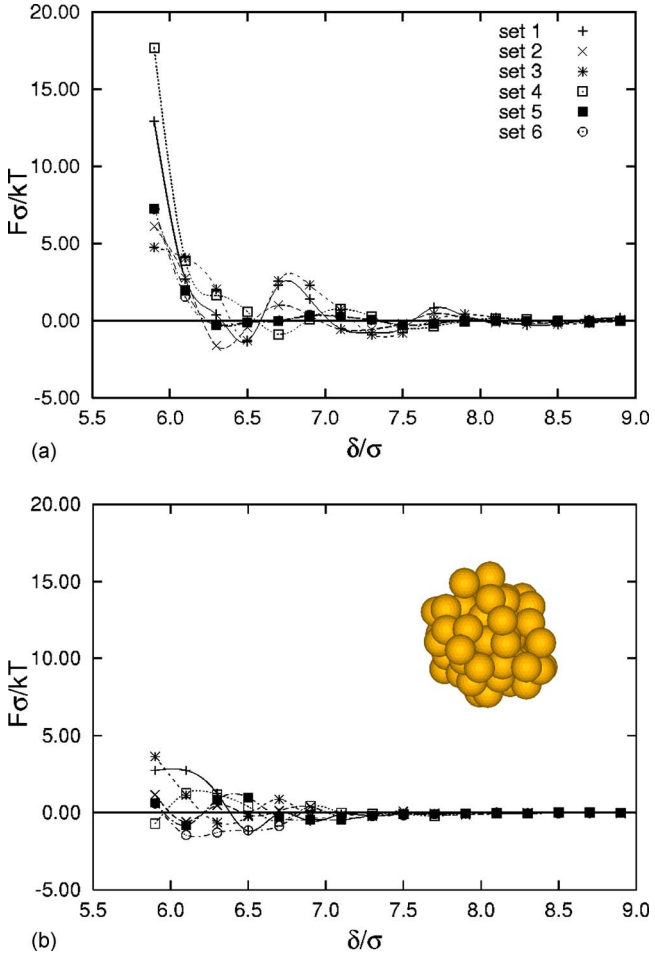

FIG. 2. (Color online) Solvation-force profiles for the rough spherical nanoparticles [see the inset of (b)] fixed at their initial configurations (a) and freely rotating about their centers of mass (b) under the impact of solvation forces and beginning with their initial configuration in (a).

tion and rigid-body rotation of the nanoparticles about their centers of mass at a fixed center-of-mass separation. Solvent motion is simulated using a second-order Gear's predictor-corrector method with a time step of 2 fs. Nanoparticle rigid-body rotation is handled by the quaternion method [29]. During the simulations, we evaluate the solvation force $F^S(\delta)$ at different center-of-mass separations δ using

$$F^S(\delta) = \langle \hat{r}_{AB}(\hat{F}_{AF} - \hat{F}_{BF}) \rangle_\delta, \tag{1}$$

in which $\hat{F}_{AF}(\delta)$ and $\hat{F}_{BF}(\delta)$ are the fluid forces on particles A and B, and $\hat{r}_{AB}$ is the unit vector pointing from the center of mass of A to that of B [i.e., $\hat{r}_{AB}=(\hat{r}_B-\hat{r}_A)/|\hat{r}_B-\hat{r}_A|$]. Solvation forces are obtained as ensemble averages from single simulation runs ranging from 1–2 ns in duration.

Figures 1 and 2 show the force profiles for the crystalline and spherical nanoparticles, respectively. The center of mass separations are different in these figures because the particles are different sizes. However, the interparticle gap separations of the different particles cover the same range of values.

Figures 1(a) and 2(a) show solvation-force profiles for nanoparticles at fixed orientations relative to one another. In these figures, it can be seen that the force profile for any fixed orientation is an oscillatory function of nanoparticle separation, similar to what has been seen in experimental SFA studies involving macroscopic surfaces [2,3,5–9]. Although the solvation forces appear to span different magnitudes for the two different particles, we have determined that these discrepancies arise from differences in the particle sizes and densities. The quantity $F^S/D\rho_s^2$, where D is the equivalent sphere diameter and ρ_s is the solid density, is essentially the same magnitude for both types of particles at the same interparticle gaps, consistent with the Derjaguin approximation [1]. In fact, our earlier studies indicate that the solvation forces for the rough, spherical nanoparticles on a per area basis are comparable in magnitude to those between flat and perfect surfaces [24]. Although these results appear to contradict those seen in SFA experiments (which indicate that surface roughness diminishes solvation forces), we note that the interparticle region is significantly smaller in our simulations than that in experiments. Fluid density-functional theory and simulation studies show that the net solvation

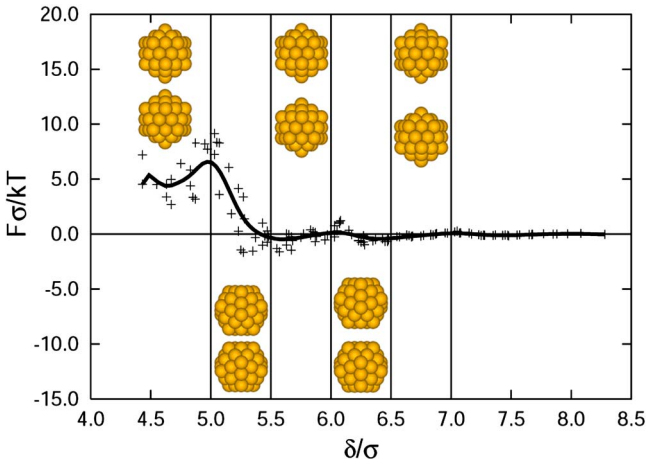

FIG. 3. (Color online) The rotational preferences of the crystalline nanoparticles along with the the force profile. The crosses are a replot of Fig. 1(b) and the solid line indicates the overall trend.

forces between rough surfaces can be viewed as a superposition of local solvation-force profiles that arise from various structural features and that this superposition reduces solvation forces [14,17]. In our study, the interparticle region is so small that such a superposition cannot be applied and the interparticle forces retain their strength.

An interesting aspect of the various force profiles in Figs. 1(a) and 2(a) is that the force profiles for different nanoparticle orientations are phase shifted relative to one another, so that the solvation forces at a fixed center-of-mass distance can be attractive for some particle orientations and repulsive for others. This suggests that if nanoparticles are allowed to freely rotate, they will select orientations that will minimize the free energy and reduce the solvation forces. By comparing Fig. 1(a) with 1(b) and Fig. 2(a) with 2(b), we see that the solvation forces are lowered dramatically when rotation is allowed and that there is less variation between the different force profiles. In experimental studies with the SFA and AFM, it has been found that repulsive solvation forces can be greater than van der Waals attraction [2,3]. Figures 1 and 2 show that nanoparticle rotation can diminish solvation forces considerably.

The rotation of the nanoparticles is not completely random, as we would expect for Brownian motion, but directed toward particular separation-dependent configurations. This is especially evident for the crystalline nanoparticles, which, regardless of their initial configuration, always rotate to a fixed configuration that is dependent only on their separation. These configurations represent free-energy minima and the particles exhibit only small-scale vibrations about the minima once they are achieved. Figure 3 shows these preferred configurations along with their associated solvation forces. From Fig. 3 we see that the force profile can be divided into six regions with face-face and vertex-vertex alignments appearing alternately. Orientational preferences can be observed for separations up to $\delta=7.0\sigma$ and after that, the solvation forces are too small to influence particle alignment. We have also observed rotational preferences for the rough nanoparticles. However, because of the low symmetry of these nanoparticles, it is unclear whether the observed relative orientations are local or global minima.

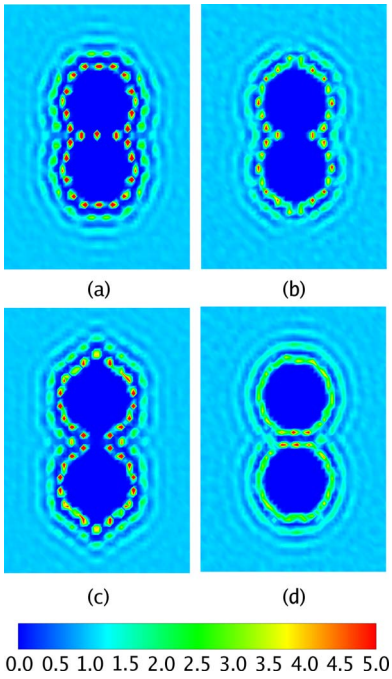

FIG. 4. (Color online) Normalized density profiles (the normalized bulk density is 1.0) at selected nanoparticle separations. (a) A fixed face-face configuration at a separation of $\delta=4.63\sigma$; (b) corresponding average rotational density profile of (a), which assumes a vertex-vertex orientation; (c) a fixed vertex-vertex configuration with a separation of $\delta=6.08\sigma$; (d) the average rotational density profile of (c), which assumes a face-face configuration.

It is noteworthy that the rotation of the nanoparticles from their initial configurations to the preferred configurations is faster than Brownian rotation. Considering the Brownian rotation of a spherical nanoparticle, which is described by $\langle\phi^2\rangle=2D_rt$, where ϕ is the rotational angle, D_r is the rotational diffusion coefficient, and t is time, the rotational diffusion coefficient D_r can be calculated by $D_r=k_BT/(8\pi\mu a^3)$, where k_B Boltzmann's constant, T is temperature, μ is the shear viscosity, and a is the sphere radius. For the conditions of our simulations [30], a free nanoparticle should rotate about 19.2° in 1 ns. However, both the crystalline and spherical nanoparticles rotate ~90° to their equilibrium positions within 0.01 to 1 ns. Faster rotational times are associated with higher initial forces. Thus, the rotation is directed for these particles. Since nanoparticles tend to be trapped in attractive minima or repelled from repulsive barriers when their alignment is not optimal, we expect them to align rapidly on the time scale of their approach, so that they maintain their equilibrium orientations.

Figure 4 illustrates the fluid density profiles around the icosahedral nanoparticles for two different sets of orientations in Fig. 1. These profiles are obtained in a slice of the simulation box centered around the plane defined by the vectors connecting the nanoparticle centers of mass and a high-symmetry direction in the relative orientation of the nanoparticles. Figures 4(a) and 4(c) show the density profiles for particles fixed at the face-face and vertex-vertex configurations at $\delta=4.63\sigma$ and 6.08σ, respectively, while Figs. 4(b) and 4(d) show profiles after the nanoparticles in (a) and (c)

have rotated to their preferred orientations, respectively. Layering of the fluid can be observed around and between the nanoparticles in Fig. 4 and we see that there is strong solidlike ordering of the fluid in the interparticle gap in (a) and (c) and that the fluid ordering and density are reduced in the preferred configurations of (b) and (d). In computer simulation studies of the SFA, attractive solvation forces have been linked to fluidlike ordering in the gap region, while repulsion has been associated with solidlike configurations [11–13]. Our studies show that particles with freedom to rotate in a solution will adjust their relative orientation to achieve fluidlike ordering in the gap.

In conclusion, we find that solvation forces can influence the alignment of nanoparticles in colloidal suspensions. For nanocrystals possessing high symmetry, the alignment effects are particularly evident and could be beneficial for colloidal nanoparticle assembly. For example, the phases and packing of nanocrystalline gold arrays has been an area of intense interest [31,32] and the results presented here indicate that solvent could be beneficial for achieving certain phases. Similarly, theoretical studies of solvated proteins [25] and polymers [27] indicate that solvent ordering and solvation forces are different when the macromolecules approach one another with different orientations. Such differences could lead to directed alignment similar to that observed here. It also seems possible that directed alignment could be influenced by solvent geometry and interactions, leading to various possible nanoparticle orientations dictated by solvent choice. The existence of these separation-dependent preferences indicate a new level of molecular insight to the solvation force and the self-assembly of nanoparticles in solution.

This work was funded by an EPA Star Grant program, Grant No. R-8290501, the Petroleum Research Fund of the American Chemical Society, and the NSF, Grant No. CCR-0303976.

[1] J. N. Israelachvili, *Intermolecular & Surface Forces*, 2nd ed. (Academic, San Diego, 1992).
[2] R. G. Horn and J. N. Israelachvili, J. Chem. Phys. **75**, 1400 (1981).
[3] H. K. Christenson, J. Chem. Phys. **78**, 6906 (1983).
[4] H. K. Christenson, J. Chem. Phys. **90**, 4 (1986).
[5] J. N. Israelachvili, Surf. Sci. Rep. **14**, 109 (1992).
[6] S. J. O'Shea, M. E. Welland, and T. Rayment, Appl. Phys. Lett. **60**, 2356 (1992).
[7] R. Lim and S. J. O'Shea, Phys. Rev. Lett. **88**, 246101 (2002).
[8] M. Heuberger and M. Zäch, Langmuir **19**, 1943 (2003).
[9] Y. Zhu and S. Granick, Langmuir **19**, 8148 (2003).
[10] E. E. Meyer, Q. Lin, T. Hassenkam, E. Oroudjev, and J. N. Israelachvili, Proc. Natl. Acad. Sci. U.S.A. **102**, 6839 (2005).
[11] I. K. Snook and W. van Megen, J. Chem. Phys. **72**, 2907 (1980).
[12] J. Gao, W. D. Luedtke, and U. Landman, Phys. Rev. Lett. **79**, 705 (1997).
[13] J. C. Wang and K. A. Fichthorn, J. Chem. Phys. **108**, 1653 (1998).
[14] L. J. D. Frink and F. van Swol, J. Chem. Phys. **108**, 5588 (1998).
[15] J. P. Gao, W. D. Luedtke, and U. Landman, Tribol. Lett. **9**, 3 (2000).
[16] F. Porcheron, M. Schoen, and A. H. Fuchs, J. Chem. Phys. **116**, 5816 (2002).
[17] C. Ghatak and K. G. Ayappa, J. Chem. Phys. **120**, 9703 (2004).
[18] K. A. Dill, Biochemistry **29**, 7133 (1990).
[19] K. Lum, D. Chandler, and J. D. Weeks, J. Chem. Phys. **103**, 4570 (1999).
[20] D. Huang and D. Chandler, Proc. Natl. Acad. Sci. U.S.A. **97**, 8324 (2000).
[21] X. Huang, C. J. Margulis, and B. J. Berne, Proc. Natl. Acad. Sci. U.S.A. **100**, 11953 (2003).
[22] P. Ball, Nature (London) **423**, 25 (2003).
[23] T. Koishi *et al.*, Phys. Rev. Lett. **93**, 185701 (2004).
[24] Y. Qin and K. A. Fichthorn, J. Chem. Phys. **119**, 9745 (2003).
[25] Y.-K. Cheng and P. J. Rossky, Nature (London) **392**, 696 (1998).
[26] P.-L. Chau, Mol. Phys. **99**, 1289 (2001).
[27] L. J. D. Frink and A. D. Salinger, Langmuir **19**, 182 (2003).
[28] J. A. Northby, J. Chem. Phys. **87**, 6166 (1987).
[29] H. Goldstein, *Classical Mechanics*, 2nd ed. (Addison-Wesley, Reading, 1980).
[30] K. Meier, A. Laesecke, and S. Kabelac, J. Chem. Phys. **121**, 3671 (2004).
[31] W. D. Luedtke and U. Landman, J. Chem. Phys. **100**, 13323 (1996).
[32] R. L. Whetten *et al.*, Acc. Chem. Res. **32**, 397 (1999).